OPTIMAL TUNING OF RST CONTROLLER USING PSO OPTIMIZATION FOR SYNCHRONOUS GENERATOR BASED WIND TURBINE

K. TAHIR C. BELFEDAL T. ALLAOUI
Department of Electrical Engineering, L2GEGI Laboratory, Ibn Khaldoun University, Tiaret, Algeria
tahir.khalfallah@univ-tiaret.dz, allaoui@univ-tiaret.dz, b-cheikh@univ-tiaret.dz

M. DOUMI
Department of Electrical Engineering, CAOSEE Laboratory, Tahri Mohammed University, Bechar, Algeria
doumicanada@gmail.com

Abstract: *In this paper, we present an optimized RST controller using Particle Swarm Optimization (PSO) meta-heuristic technique of the active and reactive power regulation of a grid connected wind turbine based on a wound field synchronous generator. To continuously extract the optimal aerodynamic energy, a maximum power point tracking (MPPT) algorithm based on fuzzy logic theory is designed. The performance of the Wind Energy Conversion System (WECS) with the proposed controller is tested for fast wind speed variation using Matlab/Simulink. Simulation results demonstrated the potential of achieving maximum power tracking for the wind speed profiles considered and a considerable reduction in the torque ripples with the PSO optimized RST controller as compared to a classical controller. The results also showed a good transient response and robustness of the proposed control system.*

Key words: *Wind energy conversion systems (WECS), Particle Swarm Optimization (PSO), Wound field synchronous generator (WFSG), RST controller, Maximum Power Point Tracking (MPPT).*

1. INTRODUCTION

Electric power generation using non-conventional sources is receiving considerable attention throughout the world because of the exhaustion of fossil fuels, and environmental issue. Wind energy is a clean and inexhaustible source of energy and has become one of the fastest growing renewable energy in the world [1].

Power generation using wind energy is possible in two ways, either constant speed operation or variable speed operation. However, with the advance in power electronic converter technology, variable speed operation for wind generator is currently the most attractive because of its ability to achieve maximum efficiency at all wind velocities [2].

In WECS, several types of electric generators have been used including Squired-Cage Induction Generator (SCIG), Synchronous Generator with external field excitation, Doubly Fed Induction Generator (DFIG) and Permanent Magnet Synchronous Generator (PMSG) [3]. The primary advantage of Wound Field Synchronous Generators (WFSG) is its high efficiency because the whole stator current is used to produce the electromagnetic torque [4]. The main benefit of the WFSG with salient pole is that it allows the direct control of the power factor of the machine, consequently the stator current may be reduced under these circumstances [5].

In the last few years, many modern control techniques such as adaptive control, variable structure control and intelligent control [6, 7], have been intensively studied for controlling the nonlinear components in power systems. However, these control techniques have had few real-time applications probably due to their complex structures or the lack of confidence in their stability. The RST polynomial control, on the other hand, has a simple structure and is easy to implement. Moreover, RST is robust and is widely used in real-time applications as compared to the control techniques mentioned above. Suitable controller parameters highly improve system stability and performance. However, the online tuning of these parameters is difficult due to the complexity and highly nonlinear system dynamics [8].

A systematic design approach that leads to reduced order RST controller is desirable. Optimization theory can provide a suitable solution to deal with this complexity, especially with the availability of the powerful processing tools. The RST synthesis problem can be reformulated as an optimization problem which can be solved by various optimization techniques, given in the literature [9]. In [10, 11], optimal PI controllers were designed using PSO. Other studies have used genetic algorithms (GA) to study wind energy. A GA-based optimization technique for designing a control strategy for the converter frequency of a variable-speed wind turbine was reported in [12, 13].

This paper proposes a new approach for tuning the RST controller parameters based on the PSO meta-heuristic technique. The RST control design problem is formulated as a constrained optimization problem, which is efficiently solved based on a developed PSO algorithm [14].

The optimization problem is formulated in the form of two objective functions for tuning of stator side converter current controller parameters to get better

response of the system. The objective functions are based on the transient response characteristic parameters such as the peak overshoot ratio, rise time, peak time, settling time, set point crossing time, and steady state error.

The overall system including wind turbine, Wound Field Synchronous Generator, back to back converter, AC grid and control system of each converter has been simulated in MATLAB/SIMULINK to validate the effectiveness of the proposed control strategy.

Simulation results show that the proposed design approach is efficient to find the optimal parameters of the RST controllers and therefore improve the transient performance of the WECS over a wide range of operating conditions.

2. MODELING OF THE WIND ENERGY CONVERSION SYSTEM

The topology of the wind energy conversion system (WECS) presented in this study is depicted in Fig. 1. It consists of a wind turbine, a gearbox, a WFSG, and back-to-back converters. The rotor winding of the WFSG is connected to DC bus through a DC/DC converter, whereas the stator winding is fed by the back-to-back bidirectional Pulse Width Modulation Voltage Source Converter (PWM-VSC). The back-to-back converter consists of a generator -side converter and a grid-side converter, which are connected by a DC bus. The WECS control system consists of the generator-side control sub-system and the grid-side control sub-system. The Maximum Power Point Tracking (MPPT) algorithm is based on fuzzy logic and controls the generator side converter. The grid-side converter controller maintains the DC-link voltage at the desired level by controlling the transit of active power to the grid and the exchange of reactive power with the grid. The generator-side converter controls the power flow from the WFSG to the grid via the control of the stator currents of the direct and quadrature components of the WFSG stator current to achieve decoupled control of the active and reactive powers. The quadrature component controls the active power, whereas the direct component controls the reactive power.

2.1. Wind Turbine System

The aerodynamic power which can be extracted from the wind turbine is expressed by the following equation [15]:

$$P_a = \frac{1}{2}\rho\pi R^2 V_w^3 C_p(\lambda,\beta) \tag{1}$$

Where ρ is the air density; R is the wind turbine blade radius; V_w is the wind velocity (m/s), and C_p is called the power coefficient, which is a function of both the blade pitch angle β and the tip speed ratio (TSR) λ which is defined as

$$\lambda = \frac{R\Omega_t}{V_w} \tag{2}$$

Where Ω_t is the rotation speed of the turbine (rad/s).

The relation of C_p versus λ of a three-blade horizontal-axis wind turbine for various blade pitch angles β is illustrated in Fig. 2. The curves have been obtained by using the following equation that is commonly used in wind turbine simulators [16, 17]:

$$\begin{cases} C_p = 0.73\left(\dfrac{151}{\lambda_i} - 0.58\beta - 0.002\beta^{2.14} - 13.2\right)e^{-\frac{18.4}{\lambda_i}} \\ \lambda_i = \dfrac{1}{\dfrac{1}{\lambda - 0.02\beta} - \dfrac{0.003}{\beta^3 + 1}} \end{cases} \tag{3}$$

According to the figure, there is an optimum value of tip speed ratio λ_{opt} that leads to maximum power coefficient C_{p_max}. When $\beta=0$, the TSR in (2) can be adjusted to its optimum value with $\lambda_{opt} = 8.1$, and with the power coefficient reaching $C_{p\_max} = 0.48$.

The turbine torque is expressed as the ratio of the mechanical power to the turbine speed as follows:

$$T_a = \frac{P_a}{\Omega_t} \tag{4}$$

The mechanical equation of the shaft, including both the turbine and the generator masses, is given by:

$$J\frac{d\Omega_m}{dt} = T_m - T_{em} - f\Omega_m \tag{5}$$

J and f are the total moment of inertia and the viscous friction coefficient appearing at the generator side, T_m is the gearbox torque, T_{em} is the generator torque, and Ω_m is the mechanical generator speed.

The wind turbine shaft is connected to the WFSG rotor through a gearbox which adapts the slow speed of the turbine to the WFSG speed. This gearbox is modeled by the following equations:

$$\Omega_t = \frac{\Omega_m}{G} \tag{6}$$

$$T_m = \frac{T_a}{G} \tag{7}$$

G is the gear ratio.

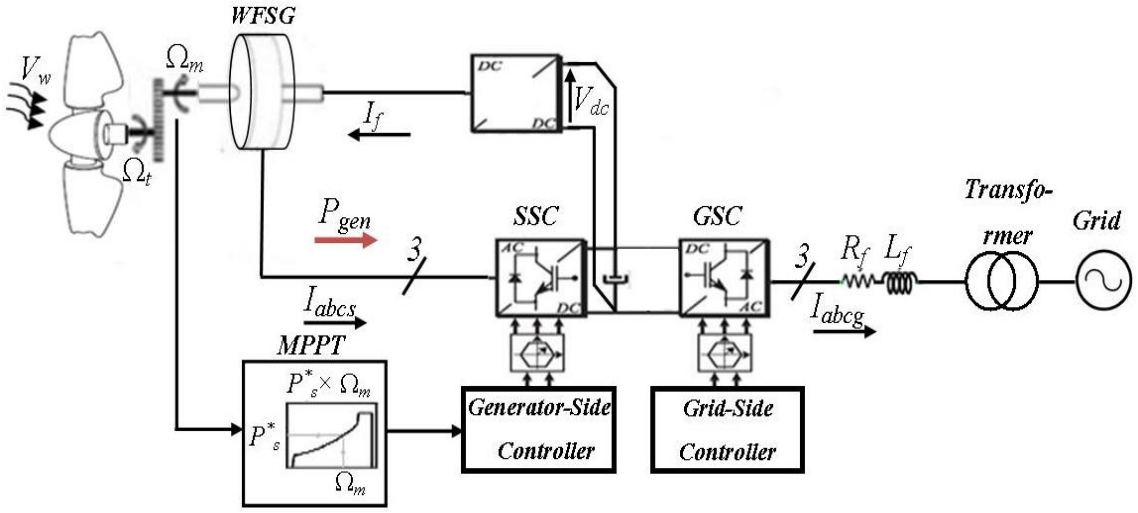

Fig. 1. Wind energy conversion system structure.

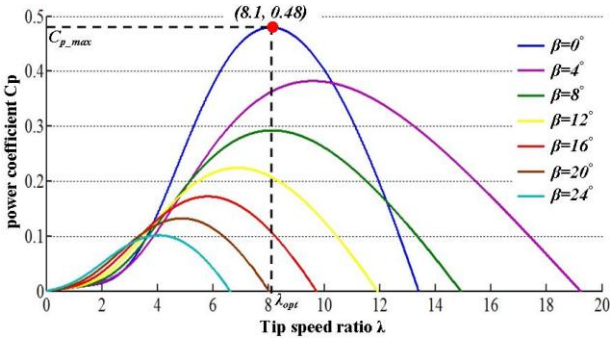

Fig. 2. Power coefficient versus tip speed ratio.

3.2. Synchronous generator modeling

In the synchronous *d-q* coordinates, the voltage equation of the WFSG is expressed as follows [18]:

$$v_{ds} = -r_s i_{ds} + \omega_e L_q i_{qs} - \omega_e M_{sQ} i_Q - L_d \frac{di_{ds}}{dt} + M_{sf} \frac{di_f}{dt} + M_{sD} \frac{di_D}{dt} \quad (8)$$

$$v_{qs} = -r_s i_{qs} - \omega_e L_d i_{ds} + \omega_e M_{sf} i_f + \omega_e M_{sD} i_D - L_q \frac{di_{qs}}{dt} + M_{sQ} \frac{di_Q}{dt} \quad (9)$$

$$v_f = -r_f i_f + L_f \frac{di_f}{dt} - M_{sf} \frac{di_d}{dt} + M_{fD} \frac{di_D}{dt} \quad (10)$$

$$0 = r_D i_D + M_{fD} \frac{di_f}{dt} - M_{sD} \frac{di_d}{dt} + L_D \frac{di_D}{dt} \quad (11)$$

$$0 = r_D i_D + M_{fD} \frac{di_f}{dt} - M_{sD} \frac{di_d}{dt} + L_D \frac{di_D}{dt} \quad (12)$$

With v_{ds}, v_{qs}, i_{ds} and i_{qs} are voltages and currents in *d-q* frame; v_f and i_f are voltage and current of the main field winding; i_D and i_Q are direct and quadrature dampers currents; r_s is stator resistance; r_f is main field resistance; r_D, r_Q are the dampers resistances; L_d and L_q represent the direct and quadrature stator main inductances; L_D and L_Q are the direct and quadrature dampers inductances; L_f is the main field inductance; M_{sf} is mutual inductance between direct stator winding and main field one; M_{fD} is the mutual inductance between main field winding and direct damper one; M_{sQ} is the mutual inductance between the stator and quadrature damper; M_{sD} is the mutual inductance between stator and direct damper; Finally, ω_e denotes the electrical angular speed of the SG, and is given by

$$\omega_e = p\Omega_m \quad (13)$$

The electromagnetic torque is expressed by:

$$T_{em} = p\left(\phi_{ds} i_{qs} - \phi_{qs} i_{ds}\right) = p[(L_q - L_d) i_{ds} i_{qs} + (M_{sf} i_f + M_{sD} i_D) i_{qs} - M_{sQ} i_Q i_{ds}] \quad (14)$$

3. MAXIMUM POWER POINT TRACKING

Since the wind profile in unknown, a simple MPPT controller based on fuzzy logic is proposed to extract maximum power from the wind turbine. The fuzzy rules are based on the variation of the wind power measured at the DC-link ΔP_a, and the rotational speed of the turbine ($\Delta\Omega_m$) [19]. The block diagram of the proposed fuzzy logic based MPPT is shown in Fig. 3.

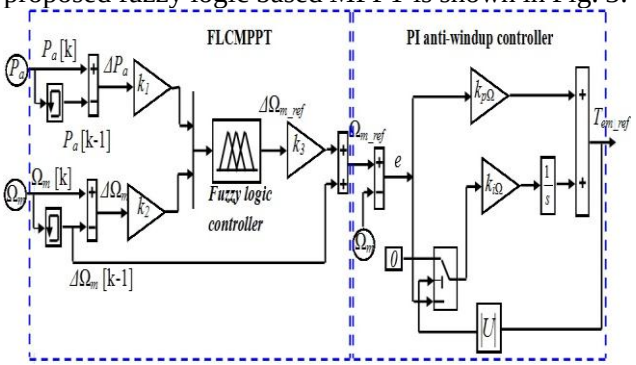

Fig. 3. Structure of MPPT fuzzy controller.

The control rules are given in Table 1, where (ΔP_a) and ($\Delta\Omega_m$) are the inputs, and ($\Delta\Omega_{m\_ref}$) represents the output. The membership functions for the inputs and

output variables are shown in Fig. 4. The linguistic terms used for the membership functions are labeled as GN (Grand Negative), N (Negative), ZR (Zero), P (Positive), GP (Grand Positive). From these linguistic rules, the FLC proposes a variation of the reference speed ($\Delta\Omega_{m\_ref}$) according to:

$$\begin{cases} \Delta P_a = P_a[k] - P_a[k-1] \\ \Delta\Omega_m = \Omega_m[k] - \Omega_m[k-1] \\ \Omega_{m\_ref}[k] = \Omega_m[k-1] + \Delta\Omega_{m-ref}[k] \end{cases} \quad (15)$$

Where $P_a[k]$ and $\Omega_m[k]$ are the rotor power and rotational speed at sampled times (k), and $\Omega_{m\_ref}[k]$ is the instant of reference speed.

As explained previously, the FLC optimizes the reference speed Ω_{m_ref} for maximum power tracking. This speed represents a positive input (reference) of the PI anti-windup controller as shown in Fig. 3, which performs the speed control in steady state. The PI anti-windup loop operates with a fast rate and provides fast response and enhances the overall system stability.

Table 1 Fuzzy rules.

$\Delta\Omega_m$	ΔP_a				
	GN	ZR	GP	P	N
N	GN	N	P	ZR	N
GP	ZR	GP	GP	GP	N
GN	GN	GN	ZR	N	GN
P	N	P	GP	P	ZR
ZR	N	ZR	P	P	N

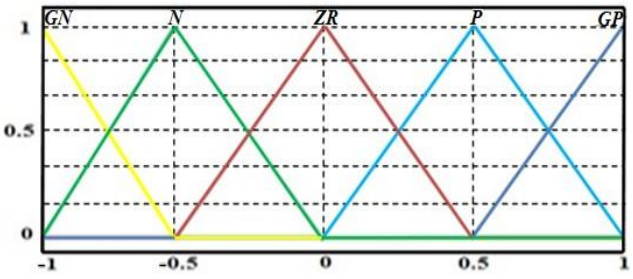

Fig. 4. Membership functions of e, ec and DU.

4. CONTROL OF GENERATOR SIDE CONVERTER

5.1. Current vector control

We have adopted the field-oriented control (FOC) principle for the torque control. By canceling the direct current i_{ds}, a simple power control can be achieved by only controlling the quadrature current [20].

Under this condition, the electromagnetic torque is given by

$$T_{em} = p.i_{qs}\left(M_{sf}i_f + M_{sD}i_D\right) \quad (16)$$

The reference signals i_{qs_ref} and i_{f_ref} are derived from (16) as follows:

$$i_{qs\_ref} = \frac{T_{em\_ref}}{p.\left(M_{sf}i_f + M_{sD}i_D\right)} \quad (17)$$

$$i_{f\_ref} = \frac{T_{em\_ref}}{p.m_{sf}i_{qs\_ref}} - \frac{M_{sD}i_D}{M_{sf}} \quad (18)$$

The decoupled control strategy of d and q current loops is obtained by rewriting (8) and (9) as:

$$v_{ds} = -\left(r_s i_{ds} + L_{ds}\frac{di_{ds}}{dt}\right) + L_{qs}\omega_e i_{qs} - M_{sQ}\omega_e i_Q \quad (19)$$

$$v_{qs} = -\left(r_s i_{qs} + L_{qs}\frac{di_{qs}}{dt}\right) - L_{qs}\omega_e i_{ds} + M_{sf}\omega_e i_f + M_{sD}\omega_e i_D \quad (20)$$

Where the terms between bracket in (19) and (20) are treated as the state equation between the voltage and current in the d and q loops respectively.

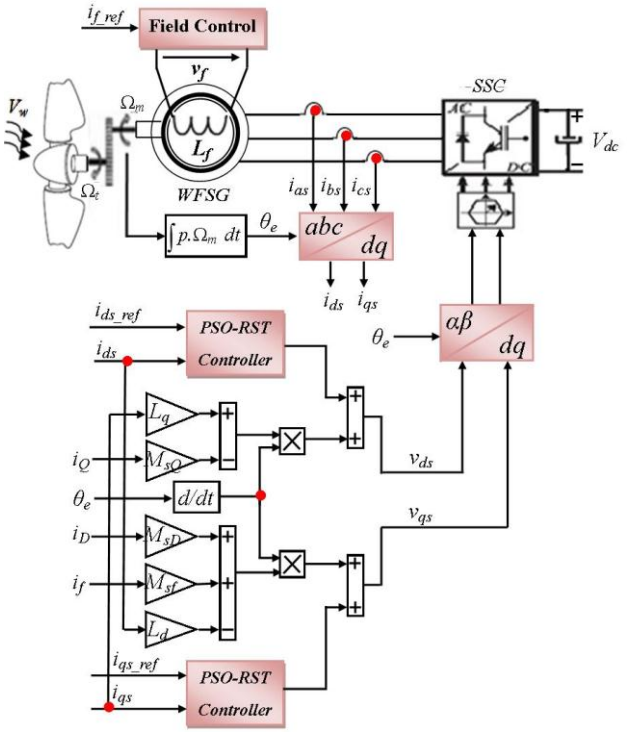

Fig. 5. WFSG vector control strategy using optimal RST controller with PSO algorithm.

The other terms are treated as either compensation or disturbance terms [21].

As depicted in Fig. 5, the control structure applied to the generator-side converter to regulate the stator

currents to their references consists of two PSO-RST controllers.

5.2. RST regulator synthesis

The RST controller is based on the robust pole placement architecture in time domain [22]. It has the advantage of solving the tradeoff between speed of response and performance as compared to proportional integral PI controller.

The block diagram of WFSG current control using a RST controller is shown in Fig. 6, where K_{PWM} is the gain of the power electronic converter, T_s is equal to one switching period, and R, S ,T are the controller polynomials. e_{ds} and e_{qs} are the d and q axial induced voltages of WFSG which act as disturbances.

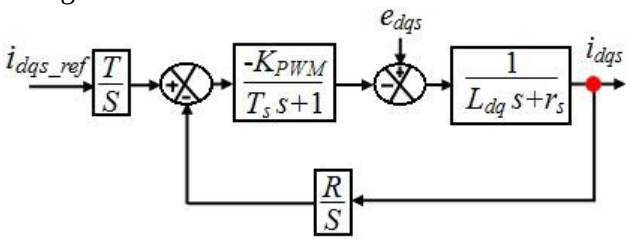

Fig. 6. Block diagram of WFSG current control using a RST controller.

The closed-loop transfer-function of the controlled system is

$$i_{dqs} = \frac{BT}{AS+BR} i_{dqs\_ref} + \frac{BS}{AS+BR} e_{dqs} \qquad (21)$$

Where A and B are defined as follows:

$$A = a_1 s + a_0 = \frac{L_{dqs}}{r_s} s + 1 \text{ and } B = b_0 = \frac{1}{r_s} \qquad (22)$$

$S(s)$ and $R(s)$ appear in the denominator of (21) and their parameters are obtained by solving the Bezout equation defined by:

$$D(s) = A(s)S(s) + B(s)R(s) \qquad (23)$$

The choice of the polynomials orders is an important step in the design of the RST controller. It is a compromise between performance and complexity of the controller structure. We choose a strictly proper controller in order to achieve a good accuracy [23, 24]. So, if A *is a* polynomial of order n ($deg(A) = n$), we must have

$$\begin{cases} \deg(D) = 2n+1 \\ \deg(S) = \deg(A)+1 \\ \deg(R) = \deg(A) \end{cases} \qquad (24)$$

Thus, polynomials $D(s)$, $R(s)$ and $S(s)$ can be written as:

$$\begin{cases} D(s) = d_3 s^3 + d_2 s^2 + d_1 s \\ S(s) = s_2 s^2 + s_1 s \\ R(s) = r_1 s + r_0 \end{cases} \qquad (25)$$

According to the robust pole placement strategy, the polynomial $D(s)$ is written as:

$$D(s) = CF = \left(s + \frac{1}{T_c}\right).\left(s + \frac{1}{T_f}\right)^2 \qquad (26)$$

With $p_c = -1/T_c$ is the pole of polynomial C and $p_f = -1/T_f$ is the double pole of the polynomial filter F.

The pole p_c must accelerate the system and is generally chosen 2–5 times greater than the pole of A. P_f is generally chosen 3–5 times smaller than p_c .

By replacing $A(s)$ and $B(s)$ from (22), (25) in the Bezout equation (23), we find:

$$\begin{aligned} D(s) &= a_1 s_2 s^3 + (a_1 s_1 + a_0 s_2) s^2 \\ &+ (a_0 s_1 + b_0 r_1) s + b_0 r_0 \end{aligned} \qquad (27)$$

The identification between (26) and (27) makes it possible to obtain the system of four equations with four unknown terms:

$$\begin{cases} a_1 s_2 = 1 \\ a_1 s_1 + a_0 s_2 = \dfrac{2}{T_f} + \dfrac{1}{T_c} \\ a_0 s_1 + b_0 r_1 = \dfrac{1}{T_f^2} + \dfrac{2}{T_c T_f} \\ b_0 r_0 = \dfrac{1}{T_c T_f^2} \end{cases} \qquad (28)$$

$T(s)$ can be a constant that guarantees zero steady-state errors. By using (21) and considering that $S(s)=0$ in steady state, $T(s)$ can be obtained as follows:

$$T(s) = t_0 = r_0 \qquad (29)$$

5.3. RST problem formulations

In this section, the design of RST controller is formulated as a constrained optimization problem which is solved using the proposed PSO approach. The choice of the adequate pole values for the RST controller is often done by a trial and error procedure.

This tuning problem becomes difficult without a systematic design method. To deal with these

difficulties, we propose to optimise these scaling factors. This problem can be formulated as the following constrained optimization problem:

$$\begin{cases} \text{minimize } f(x) \\ x \in D \\ subjectto \\ g_l(x) \le 0; \forall l = 1,....., n_{con} \end{cases} \quad (30)$$

Where the cost function *f*: $\mathbb{R}^m \to \mathbb{R}$ and the initial search space $D = \left\{ x \in \mathbb{R}^m ; x_{\min} \le x \le x_{\max} \right\}$, which is supposed to contain the desired design parameters, and $g_l : \mathbb{R}^m \to \mathbb{R}$ the problem's constraints. The optimization-based tuning problem consists of finding the optimal decision variables $x^* = \left(x_1^*, x_2^*, ..., x_m^* \right)^T$, representing the RST controller structure, which minimize the defined cost function, chosen as the Integral of squared error (ISE) and the Integral of Absolute Error (IAE) performance criteria [9].

These cost functions are minimized, using the proposed constrained PSO algorithm, under various time-domain control constraints such as overshoot *D*, steady state error E_{ss}, rise time t_r and settling time t_s of the system's step response, as shown in equation (31). Hence, in the case of RST controller structure, the poles to be optimized are (s_0, s_1,…., s_n) and (r_0, r_1,….., r_m).

The formulated optimization problem is defined as follows:

$$\begin{cases} \text{minimize } f(x) \\ x = \left(s_0, s_1, ..., s_n, r_0, r_1, ..., r_m \right)^T \in \mathbb{R}_+^k \\ subjectto \\ D \le D^{\max}; t_s \le t_s^{\max}; t_r \le t_r^{\max}; E_{ss} \le E_{ss}^{\max} \end{cases} \quad (31)$$

Where D^{max}, E_{ss}^{max}, t_r^{max} and t_s^{max} are the specified overshoot, steady state, rise and settling times respectively.

5.4. PSO algorithm

The PSO algorithm is an evolutionary computation technique developed by Kennedy and Eberhart [14], which was inspired by the social behavior of bird flocking and fish schooling [25-27].

PSO consists of a swarm of particles $x_i \ \forall i \in \left\{ 1, 2, ..., n_p \right\}$. The maximum number of particles n_p is specified by the user. The particles x_i search for an optimal solution $x^* = \arg\min f(x) \in R^m$ of a generic optimization problem (31). The position of the i^{th} particle is denoted by $x_i := \left(x_{i,1}, x_{i,2}, ..., x_{i,m} \right)^T \in \mathbb{R}^m$ and the velocity is denoted by $v_i := \left(v_{i,1}, v_{i,2}, ..., v_{i,m} \right)^T \in \mathbb{R}^m$, where $i \in \left\{ 1, 2, ..., n_p \right\}$. The position and velocity of the i^{th} particle $x_i \in \mathbb{R}^m$ is updated in each iteration, based on equations (32) and (33) for $k \in \mathbb{Z}^+$ which indicates the iteration number

$$x_i^{k+1} = x_i^k + v_i^{k+1} \quad (32)$$

$$v_i^{k+1} = w_{k+1} v_i^k + c_1 r_{1,i}^k \left(x_i^{best,k} - x_i^k \right) + c_2 r_{2,i}^k \left(x_{swarm}^{best,k} - x_i^k \right) \quad (33)$$

Where w_{k+1} is the inertia factor, c_1 is the cognitive learning rate and c_2 is the social learning rate and is pre-specified by the user. These influence the exploration and exploitation properties of the particles and must be properly chosen for faster convergence. $r_{1,i}^k$ and $r_{2,i}^k$ represent random numbers uniformly distributed in the interval $[0,1]$.

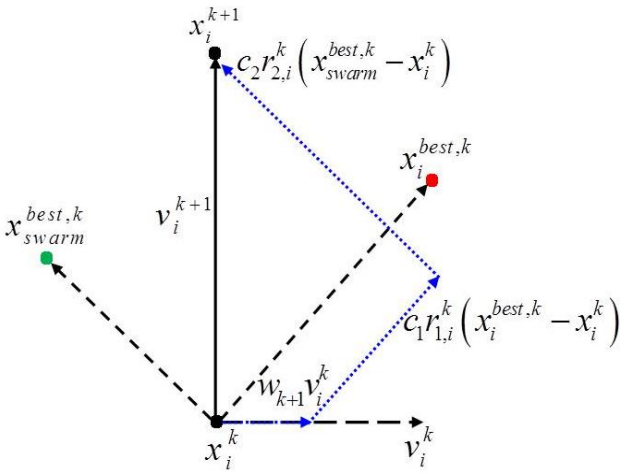

Fig. 7. Principle of particles movement in PSO.

$x_i^{best,k}$ in (34) refers to the previously obtained best position of the i^{th} particle and $x_{swarm}^{best,k}$ denotes the best position of the swarm at the current iteration k.

This is expressed as follows:

$$x_i^{best,k} := \arg\min_{x_i^j} \left\{ f(x_i^j), 0 \le j \le k \right\} \quad (34)$$

$$x_{swarm}^{best,k} := \arg\min_{x_i^k} \left\{ f(x_i^k), \forall i \right\} \quad (35)$$

Fig. 7 illustrates the principle of particles movement in PSO.

In order to improve the exploration and exploitation capacities of the proposed PSO algorithm, we chose as the inertia factor a linear evolution with respect to the algorithm iteration as given in [28]:

$$w_{k+1} = w_{\max} - \left(\frac{w_{\max} - w_{\min}}{k_{\max}} \right) k \quad (36)$$

Where the maximum and minimum inertia factor values are chosen as $w_{\max} = 0.9$ and $w_{\min} = 0.4$ respectively, $k_{\max}$ is the maximum iteration number. Similar to other meta-heuristic methods, the PSO algorithm is originally formulated as an unconstrained optimizer. Several techniques have been proposed to deal with constraints [29]. One useful approach is by augmenting the cost function of problem (30) with penalties proportional to the degree of constraint infeasibility. In this paper, the following external static penalty technique is used:

$$\varphi(x) = f(x) + \sum_{l=1}^{n_{con}} \lambda_l \max\left[0, g_l(x)^2\right] \quad (37)$$

Where λ_l is a prescribed scaling penalty parameter and n_{con} is the number of problem constraints $g_l(x)$.

Finally, the basic proposed PSO algorithm can be summarized by the following steps [9]:

1) Defining all PSO algorithm parameters such as swarm size n_p, maximum and minimum inertia factor values, cognitive c_1 and social c_2 learning rate, etc.
2) Initialize the n_p particles with randomly chosen positions x_i^0 and velocities v_i^0 in the search space D. Evaluate the initial population and determine $x_i^{best,0}$ and $x_{swarm}^{best,0}$.
3) Increment the iteration number k. For each particle apply the update equations. (32) and (33), and evaluate the corresponding fitness values $\phi_i^k = \phi\left(x_i^k\right)$:
   - If $\phi_i^k \le pbest_i^k$ then $pbest_i^k = \phi_i^k$ and $x_i^{best,k} = x_i^k$, else $x_i^{best,k} = x_i^{best,k-1}$.
   - If $\phi_i^k \le gbest_i^k$ then $gbest_i^k = \phi_i^k$ and $x_{swarm}^{best,k} = x_i^k$, else $x_{swarm}^{best,k} = x_{swarm}^{best,k-1}$.

Where $pbest_i^k$ and $gbest_i^k$ represent the best previously fitness of the i^{th} particle and the entire swarm, respectively.

4) If the termination criterion is satisfied, the algorithm terminates with the solution: $x^* = \arg\min_{x_i^k} \left\{ f\left(x_i^k\right), \forall i,k \right\}$. Otherwise go to step 3.

5.5. Scheduling PSO for PID controller parameters

To design the optimal RST controller, the PSO algorithms are applied to find the globally optimal parameters of the RST. The structure of the RST controller with PSO algorithms is shown in Fig 8.

In this paper, the polynomials *R(s)* and *S(s), T(s)* have the form:

$$\begin{cases} R(s) = r_1 s + r_0 \\ S(s) = s_2 s^2 + s_1 s \\ T(s) = t_0 \end{cases} \quad (38)$$

Hence the optimization problem is defined with a dimension $k = 4$.

$$\begin{cases} \text{minimize } f(x) \\ x = (s_1, s_2, r_0, r_1)^T \in \mathbb{R}_+^4 \\ f(x) = \int_0^{+\infty} |e(x)| dx \end{cases} \quad (39)$$

In order to confirm the convergence conditions and the choice of parameters of the PSO algorithm implemented, we applied the algorithm for the coefficient values of social c_1 and cognitive c_2 on the one hand, and its inertia factor w on the other hand which are shown in the table below.

Table 2
The PSO algorithm parameters

PSO Algorithm Parameters	values
c_1	1.2
c_2	1.2
$[w_{\min}, w_{\max}]$	[0.4, 0.9]

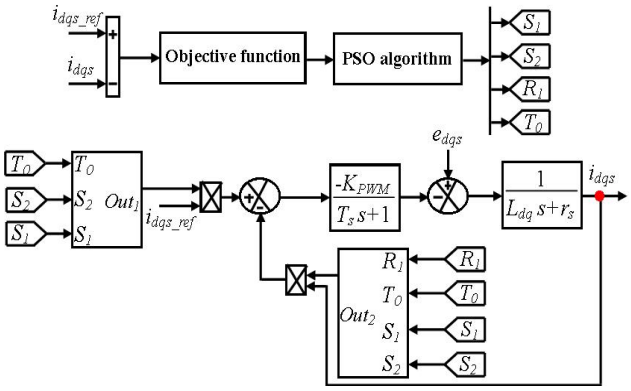

Fig. 8. The block diagram of proposed RST controller with PSO algorithm.

5. SIMULATION RESULTS AND DISCUSSION

To evaluate the performance of the proposed algorithm, a series of simulations have been performed for a 7.5 kW WFSG wind power system using Matlab Simulink™.

The parameters of the WECS are listed in Table 3 (Appendix).

6.1. Step change in wind speed

Simulation results for this case are shown in Figs. 10-15. In Fig. 9, the wind speed is shown in the form of fast step variation.

To extract maximum wind power, the power coefficient should be maintained at its optimal value. As shown in Fig. 10, the maximum power coefficient C_{p_max} value can be almost achieved, though there is an obvious drop in at t = 2 s and t = 4 s.

As shown in Fig. 11, the RST controller (with PSO algorithm) have a better tracking performance and for reference the mechanical rotation speed Ω_m than RST controller (without PSO algorithm) with smaller overshoots and quicker response at step-change wind.

From Fig. 12, it can be seen that larger overshoots occur in the current i_{qs} following a step change in the wind speed in the case of RST controller as compared to the case of RST with PSO tuning.

As shown in Fig. 15, the tracking performance of the current i_{ds} is similar for both controllers with a difference in steady state error. The torque curves T_{em} are shown in Fig. 13. From this figure, it can be seen that the generated torque reference follows the optimum mechanical torque of the turbine perfectly in the case of the proposed controller as compared to the controller RST (without PSO algorithm).

A comparison is done here with the results obtained from conventional RST controller, which also aims at torque ripple minimization. The results of the comparison are that the torque ripple is reduced considerably with the help of PSO as shown in Fig. 13.

Similarly, stator current with PSO-tuned RST controller is smooth as compared with that of standard RST controller as shown in Fig. 14. From the zoomed stator current in Fig. 14, it is clear that the stator current in classical RST has a high THD (Total Harmonic Distortion) as compared to the stator current in case of PSO technique. Table 4 (Appendix) gives a comparison of the performance between the two controllers.

6.2. Random wind speed

To complete the comparison of the two controllers tracking efficiency, a second test was performed under random wind as shown in Fig. 16.

The performance of the control strategies "RST (with PSO algorithm)" and "RST (without PSO algorithm)" has been investigated as illustrated in Figs. 17 and 18 respectively which show the (a) Power coefficient; (b) Generator speed, (c) Electromagnetic torque of the WFSG; (d) quadratic stator current, and (e) Direct stator current. As depicted from these figures, the proposed control strategy "RST (with PSO algorithm)" has a better response. The oscillations in the system states have been considerably reduced by the proposed control strategy "RST (with PSO algorithm)" as compared to the polynomial RST (without PSO algorithm).

In addition to this, the "RST (with PSO algorithm)" controller proves to have a better tracking performance for both low and the high wind speeds and when subjected to the random wind speed variation.

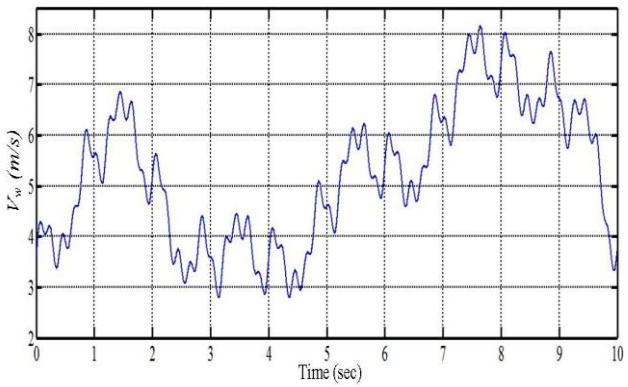

Fig. 16. Random wind speed profile.

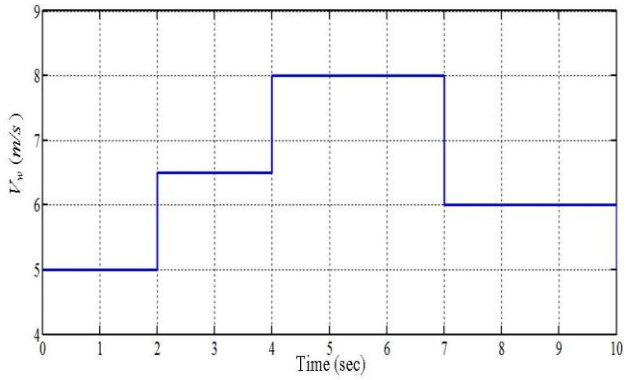

Fig. 9. Wind speed.

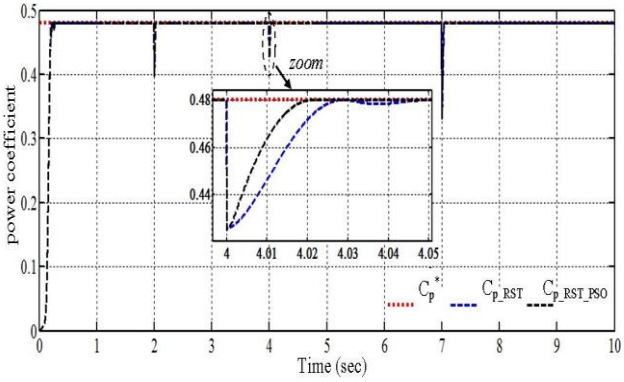

Fig. 10. Power coefficient.

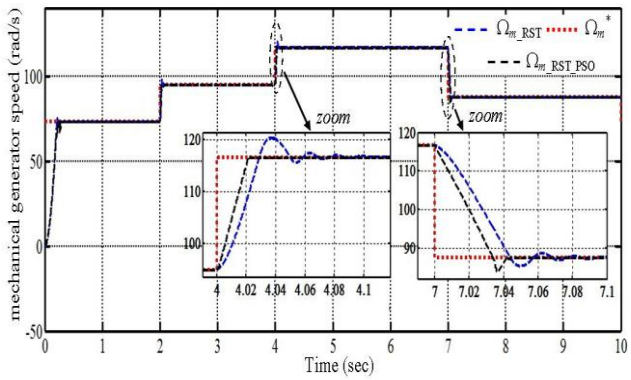

Fig. 11. Random of the WFSG rotor speed.

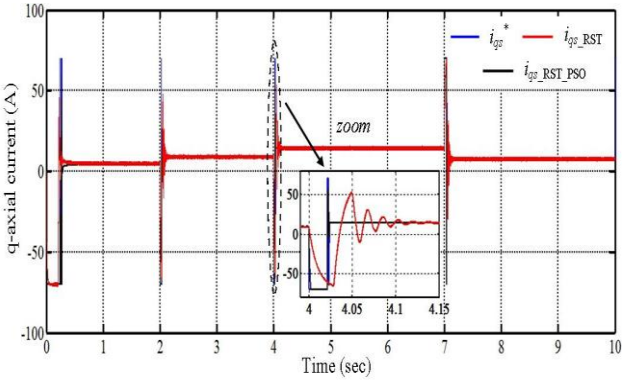

Fig. 12. Quadratic stator current.

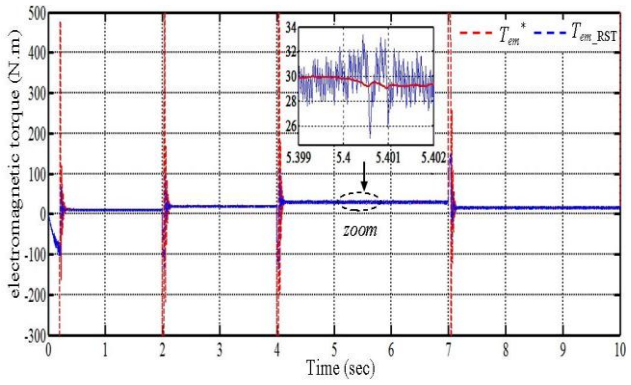

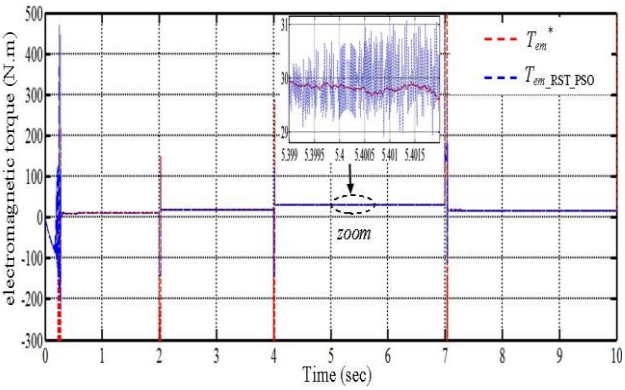

Fig. 13. Generator torque: (a) without and (b) with PSO algorithm.

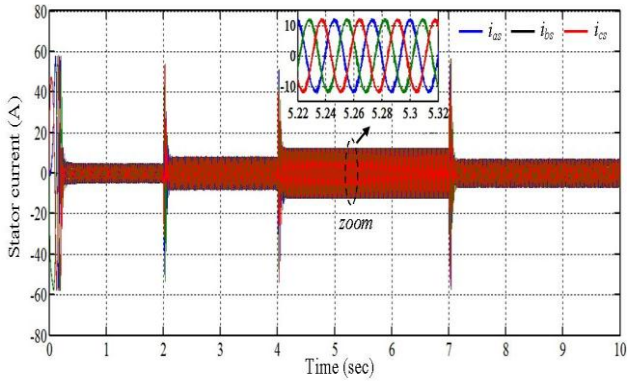

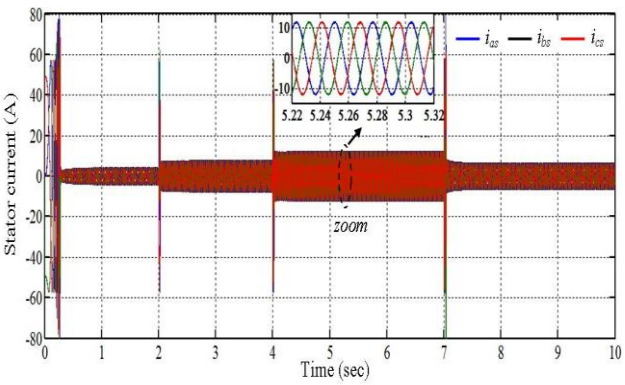

Fig. 14. Stator current: (a) without and (b) with PSO algorithm.

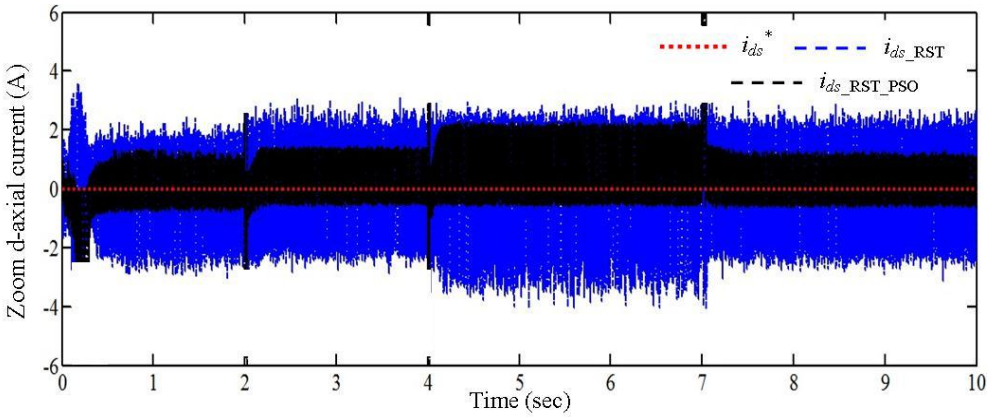

Fig. 15. Zoom of direct stator current.

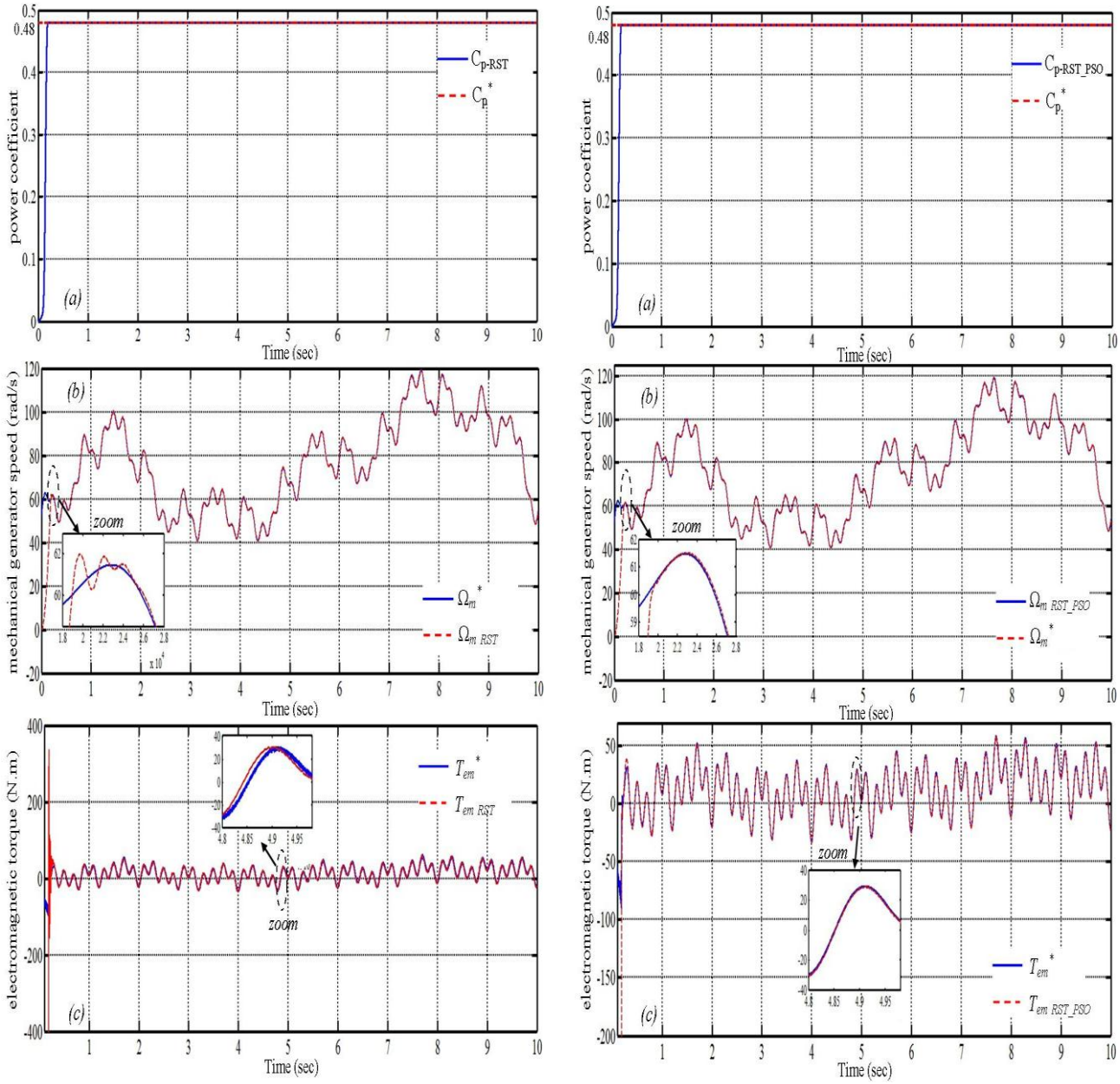

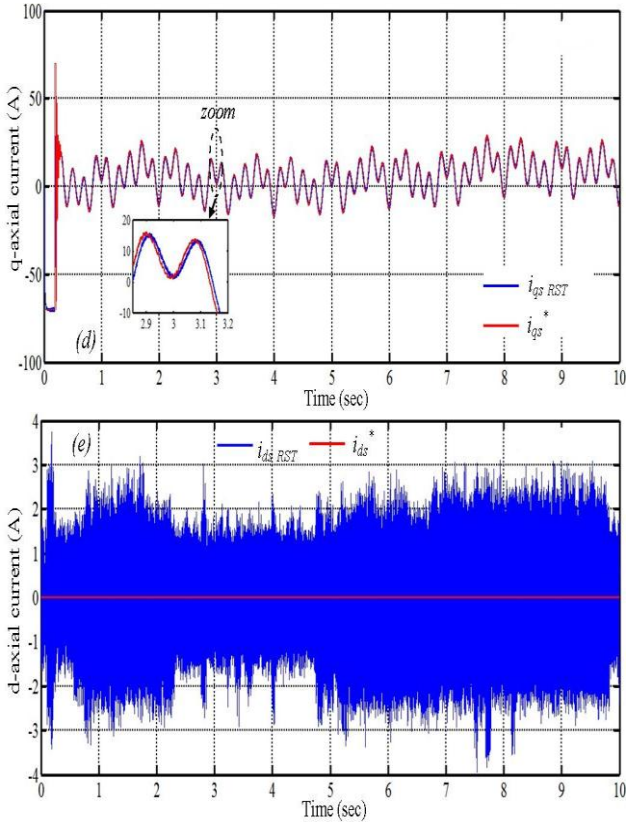

Fig. 17. System performance under random wind speed using a RST controller. (a) Power coefficient. (b) Generator speed (rad/s). (c) Generated torque (N.m). (d) Quadratic stator current (A). (e) Direct stator current (A).

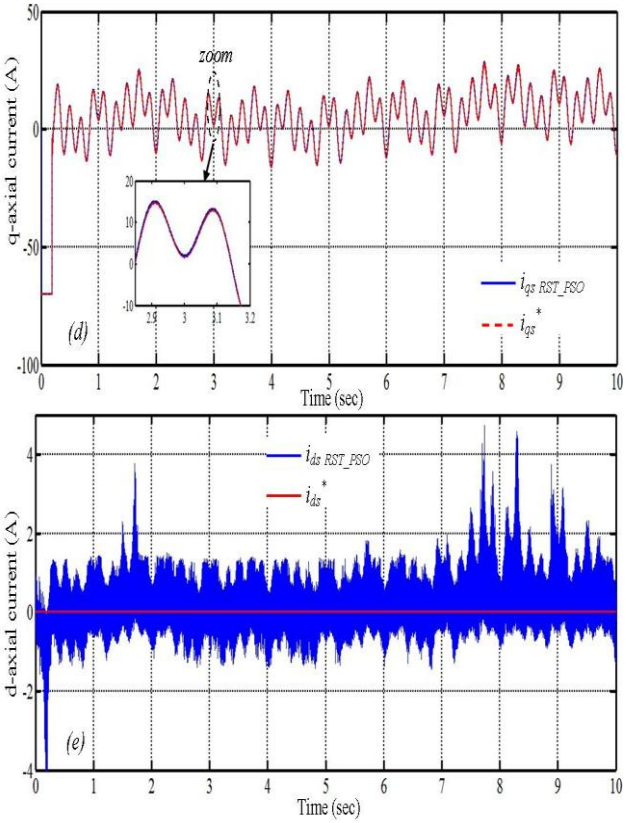

Fig. 18. System performance under random wind speed using a RST controller with PSO. (a) Power coefficient. (b) Generator speed (rad/s). (c) Generated torque (N.m). (d) Quadratic stator current (A). (e) Direct stator current (A).

6. Conclusion

In this paper we have proposed a PSO-optimised RST controller for the active and reactive power in order to minimize the ripple in the torque. The performance of this controller has been compared with a classical RST for various operating conditions. The simulation results show that the proposed controller is able to provide good response characteristics for the WECS than the traditional RST controllers. It is clear from the results that there is a reduction of ripple in torque when the proposed PSO method is used.

Appendix

Table 3
Parameters used in the simulation models

Turbine	
Rated Power the turbine P_t [KW]	10
Density area, ρ [kg.m^{-2}]	1.225
Radius of the turbine, R [m]	3
Number of blades	3
Gear ratio, G	5
Viscous friction coefficient, f [Nm.s.rad^{-1}]	0.017
WFSG	
Rated Power of the generator, S_n	7.5 KVA
Stator résistance, r_s	1.19 Ω
Rotor résistance, r_f	3.01 Ω
Phase to phase rated voltage, U_{rms}	400 V
Direct synchronous reactance, x_d	1.4 p.u
Transverse synchronous reactance, x_q	0.7 p.u
Open circuit transient time constant, T''_{do}	522 ms
Direct transient synchronous reactance, x'_d	0.099 p.u
Direct sub transient synchronous reactance, x''_d	0.049 p.u
Direct transient time constant, T'_d	40 p.u
Direct sub transient time constant, T''_d	3.7 ms
Armature time constant, T_a	6 ms

Table 4
Parameters of the RST controllers

PSO (RST) controller	S_2	S_1	r_1	r_0	D	E_{ss}	t_r	t_s
with	35	4.12e5	-4.16e7	-4.27e9	0	0.01	0.023	0.023
without	35	3.23e5	-2.58e7	-2.63e9	0.3	0.1	0.025	0.05

References

1. Senjyu, T., Tamaki, S., Muhando, E., Urasaki, N., Kinjo, H., Funabashi, T., Fujita, H., Sekine, H.: *Wind velocity and rotor position sensorless maximum power point tracking control for wind generation system*. In: Renewable Energy, Vol.31, No.11, 2006, p. 1764–1775.
2. Meharrar, A., Tioursi, M., Hatti, M., Boudghène, S.A.: *A variable speed wind generator maximum power tracking based on adaptative neuro-fuzzy inference system.* In: Expert Systems with Applications, Vol.38, 2011, p. 7659–7664.
3. Blaabjerg F., Iov L., Chen Z., Ma K.: *Power electronics and controls for wind turbine systems*. In: Proceeding IEEE of the International Conference on Energy and Exhibition, December 18-22, 2010, Manama, p. 333–344.
4. Shukla, S., Maurya, P.: *Generator and Power Converter Topology for Wind Energy Conversion System*. In: SAMRIDDHI-A Journal of Physical Sciences, Engineering and Technology, Vol.3, No.1, 2012, p. 2229–7111.
5. Topal, E., Ergene, L.: *Designing a wind turbine with permanent magnet synchronous machine*. In: IU-Journal of Electrical & Electronics Engineering, Vol.11, 2011, p. 1311-1317.
6. Calderaro, V., Cecati, C., Piccolo, A., Siano, P.: *Adaptive Fuzzy Control for Variable Speed Wind Systems with Synchronous Generator and Full Scale Converter. (Wind Power Systems: Applications of Computational Intelligence)* Springer Berlin Heidelberg, 2010, p. 337-366.
7. Rama Lingeswara Prasad, K., Chandra Sekhar, K.: *Variable Structure Controller for Generator Side Converter of Variable Speed PMSG Wind Energy Conversion System*. In: International Journal of Computer Applications, Vol.67, No.18, 2013, p. 28–33.
8. Almeida, R.G., Peas Lopes, J.A., Barreiros, J.A.L.: *Improving power system dynamic behavior through doubly fed induction machines controlled by static converter using fuzzy control*. In: IEEE Trans Power Syst, Vol.19, No.4, 2004, p. 1942–1950.
9. Bouallégue, S., Haggége, J., Benrejeb, M.: *A New Method for Tuning PID-Type Fuzzy Controllers Using Particle Swarm Optimization*. Chapter 6, p. 139-162, in Fuzzy Controllers-Recent Advances in Theory and Applications book (edited by Sohail Iqbal), InTech Education and Publishing, Rijeka, Croatia, 2012.
10. Qiao, W., Venayagamoorthy, G.K., Harley, R.G.: *Design of optimal PI controllers for doubly fed induction generators driven by wind turbines using particle swarm optimization*,". In Proceeding IEEE of the International Joint Conference on Neural Networks, Jul, 2006, Vancouver, BC, Canada, p. 1982–1987.
11. Ruiz-Cruz, R., Sanchez E.N., Ornelas-Tellez, F., Loukianov, A.G., Harley, R.G.: *Particle Swarm Optimization for Discrete-Time Inverse Optimal Control of a Doubly Fed Induction Generator*. In: IEEE Trans Cybernet, VOL. 43, No. 6, Dec 2013, p. 1698–1709.
12. Vieira, J.P.A., Nunes, M.V.A., Bezerra, U.H., Do Nascimento, AC.: *Designing optimal controllers for doubly fed induction generators using genetic algorithm*. In: IET Gener Transm Distrib, VOL. 3, No. 5, May 2009, p. 472-484.
13. Hasanien, H.M., Muyeen, S.M., *Design optimization of controller parameters used in variable speed wind energy conversion system by genetic algorithms*. In: IEEE Trans Sustain Energy, VOL. 3, No. 2, April 2012, p. 200–208.
14. Kennedy, J., Eberhart, R.: *Particle Swarm Optimization*. In: Proceedings of the IEEE International Joint Conference on Neural Networks, 27 Nov-01 Dec, 1995, Perth, WA, p. 1942-1948.
15. Beltran, B., El Hachemi Benbouzid, M., Ahmed-Ali, T.: *Second-Order Sliding Mode Control of a Doubly Fed Induction Generator Driven Wind Turbine*. In: IEEE Trans Energy Conversion, VOL. 27, No. 2, June 2012, p. 261–269.
16. Abdullah, M.A., Yatim, A.H.M., Tan, C.W., Samosir, A.S.: *Particle swarm optimization-based maximum power point tracking algorithm for wind energy conversion system* . In: Proceeding IEEE of the International Conference on power and Energy, 2-5 Dec, 2012, Kota Kinabalu, p. 65–70.
17. Mesemanolis, A., Mademlis, C., Kioskeridis, I.: *High-Efficiency Control for a Wind Energy Conversion System with Induction Generator*. In: IEEE Trans Energy Conversion, VOL. 27, No. 4, août 2012, p. 958–967.
18. Abdallah, B., Slim, T., Gérard, C., Emile, M.: *Analysis of synchronous machine modeling for simulation and industrial applications*. In: Simulation Modelling Practice and Theory, Vol.18, No.9, 2010, p. 1382–1396.
19. Abdeddaim, S., Betka, A.: Optimal tracking and robust power control of the DFIG wind turbine. In: Electrical Power and Energy Systems, Vol.49, 2013, p. 234–242.
20. Lara, O.A., Jenkins, N., Ekanayake, J., Cartwright, P., Hughes, M.: *Wind Energy Generation: Modelling and Control*. John Wiley and Sons Ltd, West Sussex, UK, 2009.
21. Jianhu, Y., Heyun, L., Yi, F., Zhu, Z.Q.: *Control of a grid-connected direct-drive wind energy conversion system*. In: Renewable Energy, Vol.66, 2014, p. 371–380.
22. Grossard, M., Boukallel, M., Chaillet, N., Rotinat-Libersa, C.: *Modeling and Robust Control Strategy for a Control-Optimized Piezoelectric Microgripper*. In: IEEE/ASME Trans Mechatronics, VOL. 16, No. 4, June 2011, p. 674–683.
23. Poitiers, F., Bouaouiche, T., Machmoum, M.: *Advanced control of a doubly-fed induction generator for wind energy conversion*. In: Electric Power Systems Research, Vol.79, No.7, 2009, p. 1085–1096.
24. Benghanem, M., Bouzid, A.M., Bouhamida, M., Draou, A.: *Voltage control of an isolated self-excited induction generator using static synchronous compensator*. In: J. Renewable Sustainable Energy, Vol.5, No.4, 2013, p. 043–118.

25. Yufei, T., Ping, J., Haibo, H., Chuan Q., Feng, W.: *Optimized Control of DFIG-Based Wind Generation Using Sensitivity Analysis and Particle Swarm Optimization*. In: IEEE Trans Smart Grid, VOL. 4, No. 1, March 2013, p. 509–520.
26. Benlahbib, B., Bouchafaa, F.: *PSO-PI Algorithm for Wind Farm Supervision*. In: Journal of Electrical Engineering, Vol.14, No.4, 2014, p. 17–23.
27. kavala k. k, vanajakshi, B.: *Optimal Design of Shunt Active Filter using Particle Swarm Optimization*. In: Journal of Electrical Engineering, Vol.14, No.4, 2014, p. 17–23.
28. Shi Y., Eberhart R.: *Empirical study of particle swarm optimization*. In: Proceedings of the Congress on Evolutionary Computation, Washington, Jul 06-09, 1999, Washington, p. 1945-1950.
29. Bouallégue S., Haggége J., Benrejeb M.: *Structured Loop- Shaping H∞ Controller Design using Particle Swarm Optimization*. In: Proceedings of the IEEE International Conference on Systems, Man, and Cybernetics SMC '10, Oct 10-13, 2010, Istanbul, p. 3563-3568.